

# On the Bandwidth of the Plenoptic Function

Minh N. Do, Davy Marchand-Maillet, and Martin Vetterli

**Abstract**—The plenoptic function (POF) provides a powerful conceptual tool for describing a number of problems in image/video processing, vision, and graphics. For example, image-based-rendering can be seen as sampling and interpolation of the POF. In such applications, it is important to characterize the bandwidth of the POF. We study a simple but representative model of the scene where bandlimited signals (e.g. texture images) are “painted” on smooth surfaces (e.g. of objects or walls). We show that in general the POF is not bandlimited unless the surfaces are flat. We then provide simple rules to estimate the essential bandwidth of the POF for this model. Our analysis reveals that, in addition to the maximum and minimum depths, the bandwidth of the POF also depend on the maximum surface slope and maximum frequency of painted signals. With a unifying formalism based on multidimensional signal processing, we can verify several key results in POF processing, such as induced filtering in space and depth correction interpolation, and quantify the necessary sampling rates.

**Index Terms**—plenoptic function, image-based rendering, sampling, spectral analysis, bandwidth.

## I. INTRODUCTION

Existing visual recording systems use a single camera, and thus provide viewers with a limited and passive viewing experience. The continuing improvement in digital technology has offered low-cost sensors and massive computing power. This has led to the development of new systems employing multiple cameras together with sophisticated processing algorithms to deliver unprecedented immersive recording and viewing capabilities. Practical systems, called *image-based rendering* (IBR) [1], that synthesize arbitrary virtual viewpoints from several fixed sensors have already emerged; see [2], [3], [4] for surveys of this area.

A natural framework for studying multiview acquisition and rendering is the concept of the *plenoptic*<sup>1</sup> *function* (POF) [5] that describes the light intensity passing through every viewpoint, in every direction, for all time, and for every wavelength. The IBR problem can be treated as an application of the sampling theory to the POF. In this setting, acquired views from the cameras provide discrete samples of the POF, and the synthesized view is reconstructed from the continuous

POF at a given point. The question of the minimum rate for sampling the POF can be addressed by spectral analysis and estimating the bandwidth of the POF.

The first sampling analysis for IBR was done by Chai et al. [6]. They analyzed the spectral support of the POF to find an optimal uniform sampling rate for the POF. Zhang and Chen [7] extended IBR sampling for more general cases, including non-Lambertian and occluded scenes. IBR sampling analysis is also reviewed in detail in a recent book [4]. In these previous studies, as for any spectral-based technique, the POF is assumed to be *bandlimited*.

In this paper, we would like to examine more precisely the spectral analysis and bandlimited assumption of the POF. To facilitate this, we study a simple but representative model where bandlimited signals (e.g. texture images) are painted on smooth surfaces (e.g. of objects or walls). Using related mathematical results on domain-warped bandlimited signals, we show that, in general, the POF is *not* bandlimited unless the surface is flat. We then provide simple rules to estimate the essential bandwidth of the POF for this model.

It is important to note that the POF is a powerful conceptual tool for describing a number of problems in image/video processing, vision, and graphics. Most acquired and synthesized forms of visual information, including images and videos, can be treated as low-dimensional “slices” (e.g. by fixing certain variables) of the POF. Hence, spectral analysis of the POF has applications beyond IBR. For example, see [8] for an application in light transport and [9], [10] for applications in computational photography.

The outline of the paper is as follows. In Section II, we set up the scene and camera models and characterize the spectral support of the POF. In Section III, we start focusing on the model in which bandlimited signals are “painted” on object surfaces. In Section IV, we discuss condition for the POF to be bandlimited. In Section V, we derive a simple rule to estimate the essential bandwidth of time-warped functions. In Section VI and Section VII, we apply this rule to estimate the essential bandwidths of the POF and the sheared (or depth corrected) POF and illustrate this with some numerical experiments. Some preliminary results of this paper were presented at a conference [11].

## II. SCENE AND CAMERA MODELS

A convenient way to parameterize the POF is to use the two-plane parameterization, also known as light field or lumigraph [12], [13], as shown in Figure 1. By restricting the scene in a bounding box, each light ray can be specified by a pair of coordinates  $(t, u)$  and  $(v, w)$  corresponding to the locations of the camera and the image pixel within a camera, respectively. Note that the image coordinate  $(v, w)$  is defined relatively with

M. N. Do is with the Department of Electrical and Computer Engineering, the Coordinated Science Laboratory, and the Beckman Institute, University of Illinois at Urbana-Champaign, Urbana IL 61801 (email: minhdo@uiuc.edu).

D. Marchand-Maillet was at the Audiovisual Communications Laboratory, École Polytechnique Fédérale de Lausanne (EPFL), CH-1015 Lausanne, Switzerland.

M. Vetterli is with the Audiovisual Communications Laboratory, École Polytechnique Fédérale de Lausanne (EPFL), CH-1015 Lausanne, Switzerland, and with the Department of Electrical Engineering and Computer Science, University of California, Berkeley CA 94720 (email: martin.vetterli@epfl.ch).

This work was supported in part by the US National Science Foundation under Grant CCR-0312432 and the Swiss National Science Foundation under Grant 20-63664.00.

<sup>1</sup>*Plenus* in Latin means complete or full.

respect to the camera position  $(t, u)$ . Hence equivalently,  $(t, u)$  specifies the viewing position and  $(u, w)$  specifies the viewing angle.

The two-plane parameterization fits the *pinhole* camera model [14], in which all pixels in a camera correspond to light rays that are emitted from one point – the camera position. The value of the plenoptic function  $p(t, u, v, w)$  is the light intensity captured by a camera at location  $(t, v)$  and at pixel location  $(v, w)$  within that camera. In general,  $p(t, u, v, w)$  is the light intensity at the intersection of the ray specified by  $(t, u, v, w)$  with the nearest object surface to the camera position  $(t, v)$ .

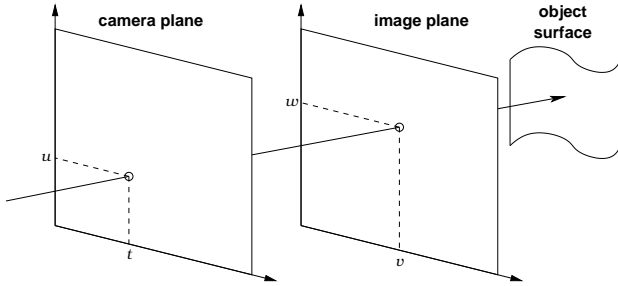


Fig. 1. The two-plane parameterization of the plenoptic function. Each light ray is specified by a 4-D coordinate  $(t, u, v, w)$ , where  $(t, u)$  corresponds to the camera location in the *camera plane* and  $(v, w)$  corresponds to the image point (or pixel) in the *image plane*. Effectively,  $(t, u)$  specifies the viewing position and  $(u, w)$  specifies the viewing angle.

For simplicity of exposition, and as in [6], [7], we consider a 2-D version of the POF,  $p(t, v)$ , by fixing  $u$  and  $w$ . This corresponds to the situation where the cameras are placed on a straight line and we consider the same image scan-line from each camera. Alternatively, we could view this as a flatland model where the 3D world is “flattened” into a 2D plane. The function  $p(t, v)$  is also known as epipolar-plane image (EPI) [15] and plays an important role in computer vision [14], [16].

We consider the scene model, as shown in Figure 2, that consists of an object surface (in the 2D setting of the POF, this a slice of the surface) specified by its varying depth  $z(t)$ . Without loss of generality, we rescale the depth value  $z$  so that the focal length or distance between the camera and image planes is equal to 1. This scene model represents a *micro-scale analysis* of the plenoptic function, where locally only one object surface is visible.

Suppose that the light ray  $(t, v)$  specified by the camera (or viewing) position  $t$  and pixel position (or viewing angle)  $v$  intersects with the object surface at a point with coordinate  $(x, z(x))$  as shown in Figure 2. Then simple geometric relations lead to

$$t = x - z(x) \tan(\theta) = x - z(x)v. \quad (1)$$

Equation (1) defines a fundamental *geometric mapping* that links a light ray  $(t, v)$  to a position  $s$  specified by  $x$  on the object surface that is “seen” by this light ray.

We assume that there is *no self-occlusion* on the object surface in the field-of-view of the cameras. This means that each light ray  $(t, v)$  within the field-of-view can intersect with at most one point on the object surface  $z(x)$ . This is equivalent

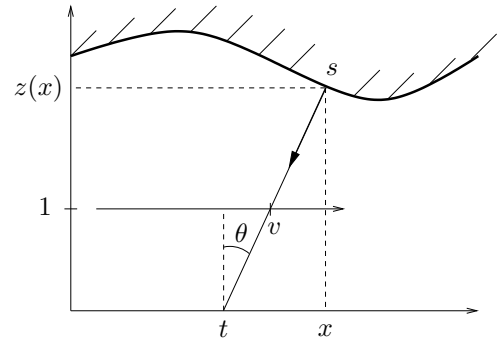


Fig. 2. Scene model with a functional surface  $z(x)$ . Coordinates  $t, v$ , and  $z$  specify the camera position, pixel position, and depth, respectively. The depth axis is rescaled so that the focal length or the distance between  $t$  and  $v$  axes is 1; and thus the pixel position  $v$  is related to the viewing angle  $\theta$  by  $v = \tan(\theta)$ .

to requiring that  $t$  given in (1) is a strictly monotonic function of  $x$ , which amounts to

$$|z'(x)| < \frac{1}{v_{\max}}, \quad (2)$$

where the field-of-view is limited by  $|v| \leq v_{\max}$ . In other words, the slope of the object surface  $z(x)$  is bounded by the maximum viewing angle.

Let  $l(x, v)$  be the light intensity emitted from the object surface position  $x$  and viewing angle  $v$  (see Figure 2). The function  $l(x, v)$  is also known as the *surface light field* [17] or *surface plenoptic function* [7]. Then using (1) and under the no self-occlusion assumption we have

$$p(t, v) = l(x, v), \quad \text{where } t = x - z(x)v. \quad (3)$$

Taking the Fourier transform of the plenoptic function  $p(t, v)$  using (3) we obtain

$$\begin{aligned} P(\omega_t, \omega_v) &\stackrel{\text{def}}{=} \mathcal{F}_{t,v}\{p(t, v)\} \\ &= \int_{-\infty}^{\infty} \int_{-\infty}^{\infty} p(t, v) e^{-j(\omega_t t + \omega_v v)} dt dv \\ &= \int_{-\infty}^{\infty} \int_{-\infty}^{\infty} l(x, v) e^{-j(\omega_t(x - z(x)v) + \omega_v v)} (1 - z'(x)v) dx dv \\ &= \int_{-\infty}^{\infty} e^{-j\omega_t x} \int_{-\infty}^{\infty} (1 - z'(x)v) l(x, v) e^{-j(\omega_v - z(x)\omega_t)v} dv dx \\ &= \int_{-\infty}^{\infty} e^{-j\omega_t x} H(x, \omega_v - z(x)\omega_t) dx, \end{aligned} \quad (4)$$

where we denote  $h(x, v) \stackrel{\text{def}}{=} (1 - z'(x)v) l(x, v)$  and  $H(x, \omega_t) \stackrel{\text{def}}{=} \mathcal{F}_v\{h(x, v)\} = \int_{-\infty}^{\infty} h(x, v) e^{-j\omega_t v} dv$ . Similarly, we denote  $L(x, \omega_v) \stackrel{\text{def}}{=} \mathcal{F}_t\{l(x, v)\}$ , and then Fourier transform properties lead to

$$H(x, \omega_v) = L(x, \omega_v) - jz'(x) \frac{\partial L(x, \omega_v)}{\partial \omega_v}. \quad (5)$$

Typically, except for rare cases of highly specular surfaces, at a fixed surface position  $x$  the emitted light intensity  $l(x, v)$  changes very slowly with respect to the viewing angle  $v$ . In the extreme case, the surface is often assumed to be *Lambertian* [16], which means  $l(x, v) = l(x)$  for all  $v$ . Thus, it is

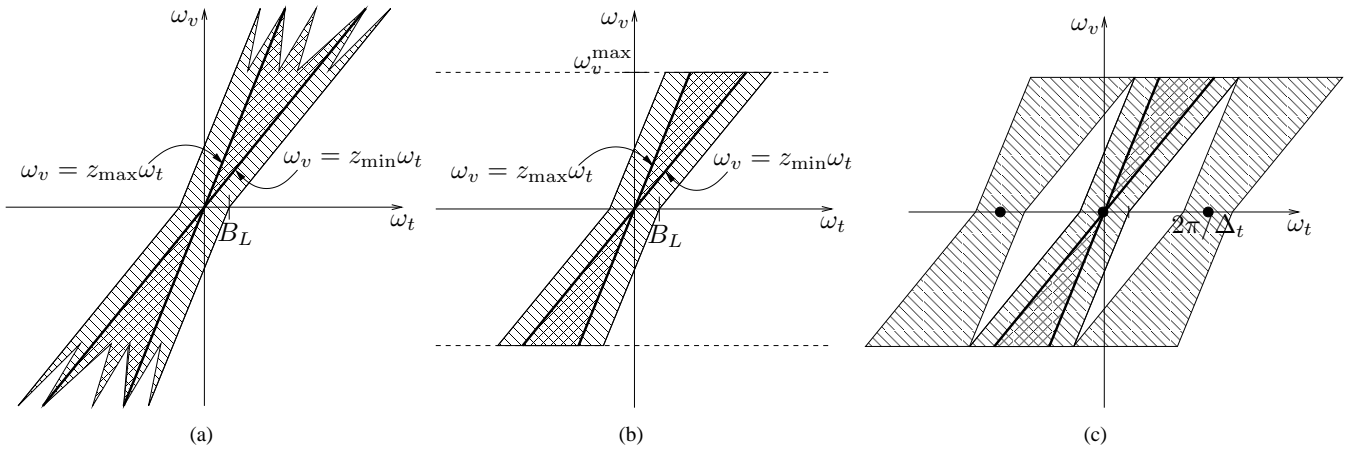


Fig. 3. The spectral supports of the plenoptic function  $p(t, v)$ . (a) The original support is contained between two lines corresponding to minimum and maximum depths, plus an extended region accounting for non-Lambertian surfaces. (b) Lowpass filtering in the pixel dimension  $v$  induces lowpass filtering in the spatial dimension  $t$ . (c) Sampling in space along  $t$  leads to periodization in frequency along  $\omega_t$ .

reasonable to assume that  $l(x, v)$  is a bandlimited function in the variable  $v$ . Using (4) and (5) we immediately obtain the following result.

*Proposition 1:* Given the no self-occlusion condition (2) and suppose that

$$L(x, \omega_v) = 0, \quad \text{if } |\omega_v| > B_L. \quad (6)$$

Then

$$P(\omega_t, \omega_v) = 0, \quad \text{if } |\omega_v - z(x)\omega_t| > B_L \text{ for all } x. \quad (7)$$

Therefore, as shown in Figure 3(a), the spectral support of the plenoptic function  $p(t, v)$  is contained between two lines corresponding to minimum and maximum depths, plus an extended region accounting for non-Lambertian surfaces. This key finding was first discovered by Chai et al. [6] for Lambertian surfaces and later extended by Zhang and Chen [7] for non-Lambertian surfaces. However, in both of these previous works the derivations are approximations based on “truncating windows”, in which the scene is approximated by piece-wise constant depth segments and the truncation effect in the spectral domain is ignored. Here, we show that for no-self-occlusion surfaces with bandlimited light radiance, the resulting POF has spectral support *exactly* contained in the region specified by (7). Moreover, our analysis reveals the role of the surface slope  $z'(x)$  as given in the second term in (5). This term was ignored in previous analyses with constant depth assumption.

This “bow-tie” shape spectral support of the POF  $p(t, v)$  makes it possible to induce *continuous-domain* lowpass filtering in the spatial dimension  $t$  via *induced filtering* in the pixel dimension  $v$ . Generally, it is physically impossible to realize continuous-domain filtering in the spatial dimension since we do *not* have access to the POF in the continuous domain of  $t$ , but rather only at discrete locations where we have actual cameras. On the other hand, continuous-domain lowpass filtering in the pixel dimension  $v$  is possible by the optical system in the cameras. Because of the “bow-tie” shape spectral support of the POF, Figure 3(b) illustrates that lowpass filtering in  $v$  induces lowpass filtering in  $t$  as well. As a result,

Figure 3(c) shows that we can sample the POF in space (i.e. by placing cameras at discrete location along  $t$ ) without alias. This induced filtering property also holds for sound signals as was shown in a study of the *plenacoustic* function [18].

Typically, the plenoptic function  $p(t, v)$  is captured by cameras with *finite pixel resolution*  $\Delta_v$  along the pixel dimension  $v$ . Thus, previous analyses [6], [7] assume that  $P(\omega_t, \omega_v)$  is bandlimited in the  $\omega_v$  dimension to  $|\omega_v| \leq \pi/\Delta_v$ . Based on this assumption and using Proposition 1 and Figure 3(b), it follows that the bandwidth of the POF depends only on the range of depths and the pixel resolution.

However, the actual continuous-domain plenoptic function  $p(t, v)$  might *not* be bandlimited according to the camera resolution. In some applications, it might be of interest to study the intrinsic bandwidth of the POF according to the underlying scene rather than the capturing devices. In this paper, we want to characterize the bandwidth of the POF  $p(t, v)$  according to a simple but representative scene model that will be described in the next section.

### III. SURFACE MODEL: SIGNALS PAINTED ON SURFACES

First, we restrict to Lambertian surfaces; i.e.  $l(x, v) = l(x)$ . Second, we assume that the light radiance  $l(x)$  is result of a bandlimited signal  $f(s)$  (e.g. texture image) “painted” on the object surface, where  $s = s(x)$  is the curvilinear coordinate (i.e.  $s$  corresponds to the arc length) on the surface. That is

$$l(x) = f(s(x)).$$

The surface coordinate  $x$  is determined by the light ray coordinate  $(t, v)$  as  $x = x(t, v)$  according to the geometric mapping equation (1) as

$$t = x(t, v) - v z(x(t, v)). \quad (8)$$

With a slight abuse of notation, we write  $s(t, v) = s(x(t, v))$  for the composite mapping from light ray coordinate  $(t, v)$  to the curvilinear coordinate  $s$  on the surface. With these mappings, we can relate the plenoptic function  $p(t, v)$  to the “painted” signal  $f(s)$  on the object surface as

$$p(t, v) = l(x(t, v)) = f(s(x(t, v))) = f(s(t, v)). \quad (9)$$

We study the bandwidth of the POF  $p(t, v)$  by fixing either  $t$  or  $v$ . Note that fixing  $t$  in the POF  $p(t, v)$  corresponds to considering an image captured by a fixed camera, whereas fixing  $v$  corresponds to considering signal recorded at a fixed pixel location by a moving camera. In both cases, we obtain a *time-warped* function of a bandlimited function  $f(s(t))$  where  $t$  and  $s$  denote a generic variable and warping function, respectively. Figure 4 depicts this generic case study of the POF.

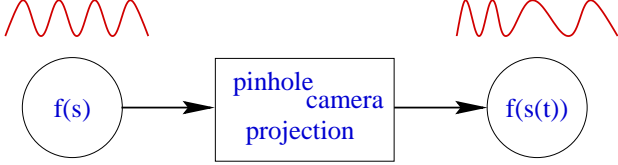


Fig. 4. Mapping from  $f(t)$  to  $(f \circ s)(t) = f(s(t))$  due to the pinhole camera projection.

Fixing either  $v$  or  $t$  and taking the derivative of (8) with respect to the other variable, we get

$$\frac{\partial x(t, v)}{\partial t} = \frac{1}{1 - v z'(x)} \quad (10)$$

$$\frac{\partial x(t, v)}{\partial v} = \frac{z(x)}{1 - v z'(x)}. \quad (11)$$

Hereafter, for brevity, in the right-hand sides we write  $x$  for  $x(t, v)$ . The no-self-occlusion condition (2) implies that both of these partial derivatives are positive for  $v \in [-v_{\max}, v_{\max}]$  or within the field-of-view. This means that  $x(t, v)$  is a strictly monotonic function in each coordinate  $t$  and  $v$ . Using differential relation  $ds = \sqrt{dx^2 + dz^2} = \sqrt{1 + (z'(x))^2} dx$ , we obtain the partial derivatives of  $s$  with respect to  $t$  and  $v$  as

$$\frac{\partial s(t, v)}{\partial t} = \frac{ds}{dx} \frac{\partial x(t, v)}{\partial t} = \frac{\sqrt{1 + (z'(x))^2}}{1 - v z'(x)} \quad (12)$$

$$\frac{\partial s(t, v)}{\partial v} = \frac{ds}{dx} \frac{\partial x(t, v)}{\partial v} = \frac{z(x) \sqrt{1 + (z'(x))^2}}{1 - v z'(x)} \quad (13)$$

From (12), we see that if the surface is flat, i.e.  $z'(x)$  is a constant then  $\partial s(t, v)/\partial t$  is a constant or  $s(t, v)$  is an affine function in  $t$  for each fixed  $v$ . Conversely, under the no-self-occlusion condition (2), if  $s(t, v)$  is affine for a fixed  $v$  then it is easy to see that  $z'(x)$  must be a constant, and thus the surface must be flat.

Finally, we note that both partial derivatives of  $s$  given in (12) and (13) are greater than 1.

#### IV. BANDLIMITED PLENOPTIC FUNCTIONS

As noted in the introduction, to address the sampling problem of the plenoptic function we need to study its spectral support. In this section, we examine the bandlimitedness of the plenoptic function given in (9). In plenoptic sampling for IBR, the main variable of interest is  $t$ , the camera position, as it leads to conditions on how to place the cameras. So let us consider the situation where the pixel position  $v$  is fixed, and for brevity we drop the variable  $v$  in functions in this section.

Again, suppose that the painted signal  $f(s)$  is bandlimited. From the discussion at the end of the last section we note that if the surface in our scene is flat, then  $s(t)$  is affine and the plenoptic function  $p(t) = f(s(t))$  is a uniformly stretched version of  $f(t)$ . Thus, it follows immediately from the shifting and scaling properties of the Fourier transform that  $f(s(t))$  is also bandlimited. We are interested to know if there are any other surfaces that result in bandlimited plenoptic functions.

Time-warped bandlimited functions have been studied in the signal processing literature. In [19], Clark conjectured that when a bandlimited function  $f$  is warped by a monotonic function  $s$ , the resulting function  $(f \circ s)(t) = f(s(t))$  is also bandlimited *if and only if*  $s(t)$  is affine. In [20], this conjecture was proved for a large class of  $s(t)$ , in particular for  $s(t)$  that on certain interval is a restriction of an entire function.<sup>2</sup> Later, in [21], Clark's conjecture was shown to be false by a peculiar counterexample constructed by Y. Meyer. However, that paper also noted that it is not possible for a non-affine warping function to preserve bandlimitedness in general. Unaware of this line of work, in [22], we made the same conjecture on the preservation of bandlimitedness under warping.

The implication of the above result is that in general, the plenoptic function is *not* bandlimited unless the surface is flat. In the next sections we will study the *essential bandwidth*, defined as the bandwidth where most of the signal energy resides, of the plenoptic function for general smooth surfaces.

#### V. BANDWIDTH OF TIME-WARPED FUNCTIONS

Let denote  $g(t) = (f \circ s)(t)$  to be a time-warped function that models the plenoptic function as was described in Section III. Its Fourier transform is

$$G(\xi) = \int_{-\infty}^{\infty} f(s(t)) e^{-j\xi t} dt. \quad (14)$$

Let  $F(\omega)$  be the Fourier transform of  $f(s)$ . Then,

$$f(s) = \frac{1}{2\pi} \int_{-\infty}^{\infty} F(\omega) e^{j\omega s} d\omega. \quad (15)$$

Substituting (15) into (14) we obtain

$$\begin{aligned} G(\xi) &= \frac{1}{2\pi} \int_{-\infty}^{\infty} F(\omega) \left( \int e^{j\omega s(t)} e^{-j\xi t} dt \right) d\omega \\ &= \frac{1}{2\pi} \int_{-\infty}^{\infty} F(\omega) K_s(\xi, \omega) d\omega, \end{aligned} \quad (16)$$

where  $K_s(\xi, \omega) \stackrel{\text{def}}{=} \mathcal{F}_t\{e^{j\omega s(t)}\}$  is the Fourier transform of  $e^{j\omega s(t)}$ . The kernel function  $K_s(\xi, \omega)$  characterizes how the warping function  $s$  broadens the spectrum of  $f$  in the warped function  $g = f \circ s$ . To see this effect, first consider the case when  $s$  is an affine function:  $s(t) = a + bt$ . In this case we have

$$K_s(\xi, \omega) = \mathcal{F}_t\{e^{j\omega(a+bt)}\} = 2\pi e^{j\omega a} \delta(\xi - b\omega), \quad (17)$$

<sup>2</sup>An entire function is a function of complex variable that has derivative at each point in the entire finite plane. In particular, bandlimited functions are entire functions.

which is concentrated along the line  $\omega = \xi/b$ . Substitute (17) into (16) we get

$$G(\xi) = \frac{e^{ja\xi/b}}{|b|} F\left(\frac{\xi}{b}\right).$$

Thus, for the affine warping  $s(t) = a + bt$  we can relate the bandwidth of the warped function  $g = f \circ s$  to the bandwidth of  $f$  as

$$\text{BW}_g = |a| \text{BW}_f = |s'| \text{BW}_f. \quad (18)$$

Next, consider a more general situation in which the warping function  $s$  deviates from an affine function as

$$s(t) = a + bt + \tilde{s}(t). \quad (19)$$

Then the kernel  $K_s(\xi, \omega)$  becomes

$$\begin{aligned} K_s(\xi, \omega) &= \mathcal{F}_t\{e^{j\omega(a+bt)} \cdot e^{j\omega\tilde{s}(t)}\} \\ &= 2\pi e^{ja\omega} \delta(\xi - b\omega) *_{\xi} \mathcal{F}_t\{e^{j\omega\tilde{s}(t)}\}. \end{aligned} \quad (20)$$

Consider a simple case where the deviation  $\tilde{s}(t)$  is an oscillation function with a single frequency  $\mu > 0$ , i.e.  $\tilde{s}(t) = c \sin(\mu t)$ . Using the following expansion

$$e^{jx \sin(\alpha)} = \sum_{n=-\infty}^{\infty} J_n(x) e^{jn\alpha},$$

where  $J_n(x)$  is the  $n$ -th order Bessel function of the first kind, we have

$$\mathcal{F}_t\{e^{j\omega c \sin(\mu t)}\} = 2\pi \sum_{n=-\infty}^{\infty} J_n(c\omega) \delta(\xi - n\mu).$$

The Bessel functions  $J_n(x)$  decay exponentially for sufficiently large  $n$  and are negligible for  $|n| > |x| + 1$ . Thus, for  $\tilde{s}(t) = c \sin(\mu t)$ , the Fourier transform  $\mathcal{F}_t\{e^{j\omega\tilde{s}(t)}\}$  is essentially zero for frequency  $|\xi| > |c\mu\omega| + \mu$ . Based on this approximation, substituting back in (20) and then (16), we see that the essential bandwidth of  $g$  is

$$\text{essBW}_g = (|b| + |c\mu|) \text{BW}_f + \mu. \quad (21)$$

Note that in this case  $s(t) = a + bt + c \sin(\mu t)$ , we can write  $|b| + |c\mu| = \max|s'|$ . Moreover, for the plenoptic function, typically the oscillation of the surface  $s$  is much smaller than the oscillation of the painted texture  $f$ , therefore  $\mu \ll \text{BW}_f$ . Furthermore, as noted at the end of Section III, for plenoptic function  $|s'| > 1$ . Thus, from (21) we can write

$$\text{essBW}_g = (\max|s'|) \text{BW}_f. \quad (22)$$

In words, the essential bandwidth of the time-warped function  $g(t) = f(s(t))$  can be approximated by the product of the maximum derivative of  $s$  with the bandwidth of  $f$ .

The rule (22) can be approximated for general warping function  $s$  as follows. Since typically  $s$  is smooth, it can be approximated by a piecewise linear function

$$\hat{s}(t) \stackrel{\text{def}}{=} s(t_k) + s'(\xi_k)(t - t_k) \quad \text{for } t \in [t_k, t_{k+1}] \quad (23)$$

with appropriately chosen  $\xi_k \in [t_k, t_{k+1}]$  and sufficiently small segments  $[t_k, t_{k+1}]$ . Then the time-warped function  $g(t) = f(s(t))$  can be approximated by

$$\begin{aligned} \hat{g}(t) &\stackrel{\text{def}}{=} f(\hat{s}(t)) \\ &= f(s(t_k) + s'(\xi_k)(t - t_k)) \quad \text{for } t \in [t_k, t_{k+1}] \\ &= \sum_k f(s(t_k) + s'(\xi_k)(t - t_k)) b_k(t), \end{aligned} \quad (24)$$

where  $b_k(t)$  is the indicator function of the interval  $[t_k, t_{k+1}]$ ; i.e.  $b_k(t)$  equals to 1 for  $t \in [t_k, t_{k+1}]$  and 0 otherwise. Denote  $f_k(t) = f(s(t_k) + s'(\xi_k)(t - t_k))$ , which is an affine warping. Then we can relate the bandwidth of  $f_k$  to the bandwidth of  $f$  as

$$\text{BW}_{f_k} = |s'(\xi_k)| \text{BW}_f.$$

Since  $b_k(t)$  is a rectangular function of length  $(t_{k+1} - t_k)$ , its Fourier transform  $B_k(\omega)$  is a *sinc* function with essential bandwidth

$$\text{essBW}_{b_k} = \frac{1}{t_{k+1} - t_k}.$$

From (25) it follows that  $\hat{G}(\omega) = \sum_k F_k(\omega) * B_k(\omega)$ , and hence

$$\text{essBW}_{\hat{g}} = \max_k \left( |s'(\xi_k)| \text{BW}_f + \frac{1}{t_{k+1} - t_k} \right). \quad (26)$$

For the plenoptic function, typically the oscillation of  $s$  is much smaller than the oscillation of  $f$ . Therefore, a good approximation of  $f(s(t))$  can be obtained from  $f(\hat{s}(t))$  using a piecewise linear approximation of  $s(t)$  as in (23) with  $\max_k 1/(t_{k+1} - t_k) \ll \text{BW}_f$ . Thus, we can discard the second term on the right-hand side of (26) and obtain

$$\text{essBW}_g \approx \text{essBW}_{\hat{g}} \approx (\max|s'|) \text{BW}_f,$$

which is the desired result (22). Note that this approximation is exact for affine warping  $s$  as shown in (18).

The bandwidth analysis of time-warped functions in this section follows the bandwidth analysis of FM (frequency-modulation) signals in communication systems [23]. A similar rule like (22) is called the Carson's rule in the communication systems literature. We note that both the Carson's rule and (22) are difficult to prove precisely, except for some particular cases, and thus they should be viewed as "rules of thumb". In the next sections, we will show that the rule (22) is quite accurate and provides an effective mean to estimate the bandwidth of plenoptic functions.

## VI. BANDWIDTH OF PLENOPTIC FUNCTIONS

The result (22) from the last section reveals the role of the maximum absolute value of the derivatives of the curvilinear coordinate  $s$  on the bandwidth of the plenoptic function. These maximum derivatives represent the worst cases of the multiplicative term in the bandwidth expansion of the POF as given in (22). From (12) and (13) we have

$$\max \frac{\partial s(t, v)}{\partial t} \leq \frac{\sqrt{1 + \max|z'|^2}}{1 - v_{\max} \max|z'|} \quad (27)$$

$$\max \frac{\partial s(t, v)}{\partial v} \leq \frac{z_{\max} \sqrt{1 + \max|z'|^2}}{1 - v_{\max} \max|z'|}. \quad (28)$$

With these maximum derivatives, together with the knowledge of the bandwidth of the painted signal (or texture image)  $f$  on the object surface, we obtain essential bandwidth estimates for the POF using (22). Intuitively, the results (27)-(28) imply that when varying camera position  $t$ , the worse case of bandwidth expansion comes from the steepest slope (with respect to the camera axis) on the object surface. When varying pixel position  $v$ , the worst case happens when the surface is at the steepest point and furthest, and the pixel is at the boundary of the field-of-view. These findings are also noted in the literature on texture mapping and image warping [24].

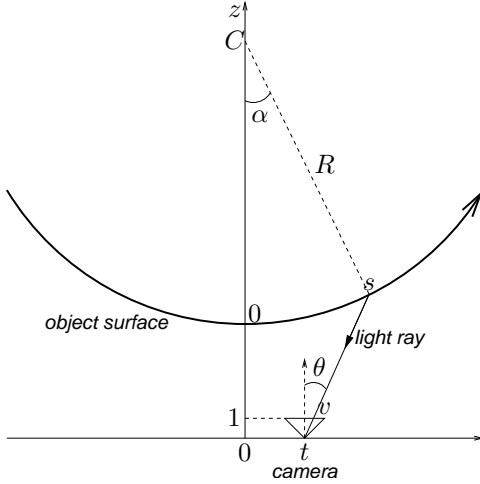


Fig. 5. The scene with a *curved wall* that is used in numerical experiments.

To illustrate and validate these rules for estimating the bandwidth of the POF we consider a synthetic scene as shown in Figure 5. Note that as before, all length measures are normalized so that the focal length (i.e. the distance between  $t$  and  $v$  axes) is equal to 1. In the scene, there is a *curved wall* as an arc of a circle with radius  $R$  and center at distance  $C$  from the origin on the  $z$  axis. A texture signal  $f(s) = \sin(2\pi\kappa s)$  of frequency  $\kappa$  is painted on the wall. For convenience, we also specify a point on the object surface by the angle  $\alpha$  between the corresponding radial line with the  $z$ -axis (see Figure 5). Then

$$\begin{cases} \frac{x}{R} = \sin(\alpha) \\ \frac{C - z(x)}{R} = \cos(\alpha) \\ s = \alpha R. \end{cases} \quad (29)$$

It follows that

$$z'(x) = \tan(\alpha).$$

Substituting (29) into the geometric mapping equation (1) and using  $\theta$  to specify the pixel position,  $v = \tan(\theta)$ , we get

$$t = R \sin(\theta) - (C - R \cos(\theta)) \tan(\theta).$$

From this we can express the curvilinear coordinate  $s$  on the object surface through the light ray coordinates  $(t, v)$  as (noting  $\theta = \tan^{-1}(v)$ )

$$s = R \left( \sin^{-1} \left( \frac{t \cos(\theta) + C \sin(\theta)}{R} \right) - \theta \right). \quad (30)$$

Figure 6(b) shows the resulting POF of a *curved wall* with  $C = 20$ ,  $R = 10$ , and  $\kappa = 2$ . The examined ranges of  $t$  and  $v$  are:  $t \in [-3, +3]$ , and  $v \in [-0.35, +0.35]$  (with the focal length normalized to 1, this is equivalent to using 50 mm lens on a 35 mm camera). With these parameters, the surface depth is in the range  $z(x) \in [10, 13.76]$  and the surface slope is in the range  $z'(x) \in [-1.25, 1.25]$ . Plugging these values into (27)-(28) and (22), we obtain the following estimates for the essential maximum frequencies of  $P(\omega_t, \omega_v)$  as

$$\begin{cases} \omega_t^{\max}/(2\pi) = 5.7Hz, \\ \omega_v^{\max}/(2\pi) = 78.6Hz. \end{cases}$$

These estimates agree well with the plot of  $P(\omega_t, \omega_v)$  for curved wall in Figure 6(d). Also note in the plot that the spectral support of the POF is sandwiched between the lines  $\omega_v = z_{\min}\omega_t$  and  $\omega_v = z_{\max}\omega_t$  as illustrated in Figure 3.

For comparison, Figure 6(a) and Figure 6(c) show the POF and its spectrum for the same camera configuration and painted texture, except the wall is *flat* at constant depth  $z(x) = 11.5$ . Comparing to the *flat wall* case, the spectrum support of the POF of the *curved wall* is significantly broader, both in the angle and the radial length of the cone-shape region illustrated in Figure 3. The angular broadening of the POF spectrum is due to the varying of surface depth  $z(x)$ , as was noted previously in [6]. However the radial broadening of POF spectrum, which is due to the maximum surface slope  $z'(x)$  as indicated in (27)-(28), is only revealed in this work.

## VII. BANDWIDTH OF SHEARED PLENOPTIC FUNCTIONS

The results in the last section characterize the bandwidths of the plenoptic function  $p(t, v)$  in each dimension  $t$  and  $v$  *separately*. For plenoptic sampling, such bandwidths are relevant if we sample and reconstruct along each dimension  $t$  and  $v$  separately while fixing the other dimension. However, the typical shapes of POF spectral supports as seen in Figure 3 and Figure 6(c-d) indicate that we can compact the POF spectrum more (and hence have less aliasing in sampling) by *non-separably* process the two dimensions  $t$  and  $v$ . In particular, using the knowledge of minimum and maximum depths,  $z_{\min}$  and  $z_{\max}$ , and the property of POF spectral support as shown in Figure 3, optimal *non-separable* reconstruction filters for IBR were derived in [6], [7].

An alternative approach to explore this property of the POF spectrum support in IBR using only 1D reconstruction filter is as follows. Since the POF spectral support is slanted according to the depth range, *shearing* the POF spectrum as shown from Figure 7(c) to Figure 7(d) would make it more compact along  $\omega_t$  axis. Figure 7(a) and Figure 7(b) illustrate the spatial supports of the corresponding functions with spectra given in Figure 7(c) and Figure 7(d); namely, the POF and its sheared version. More precisely, the desired shearing operator is obtained by the following change of variable in the frequency domain

$$\begin{cases} \omega_{t'} = \omega_t - \omega_v/z_0, \\ \omega_{v'} = \omega_v. \end{cases}$$

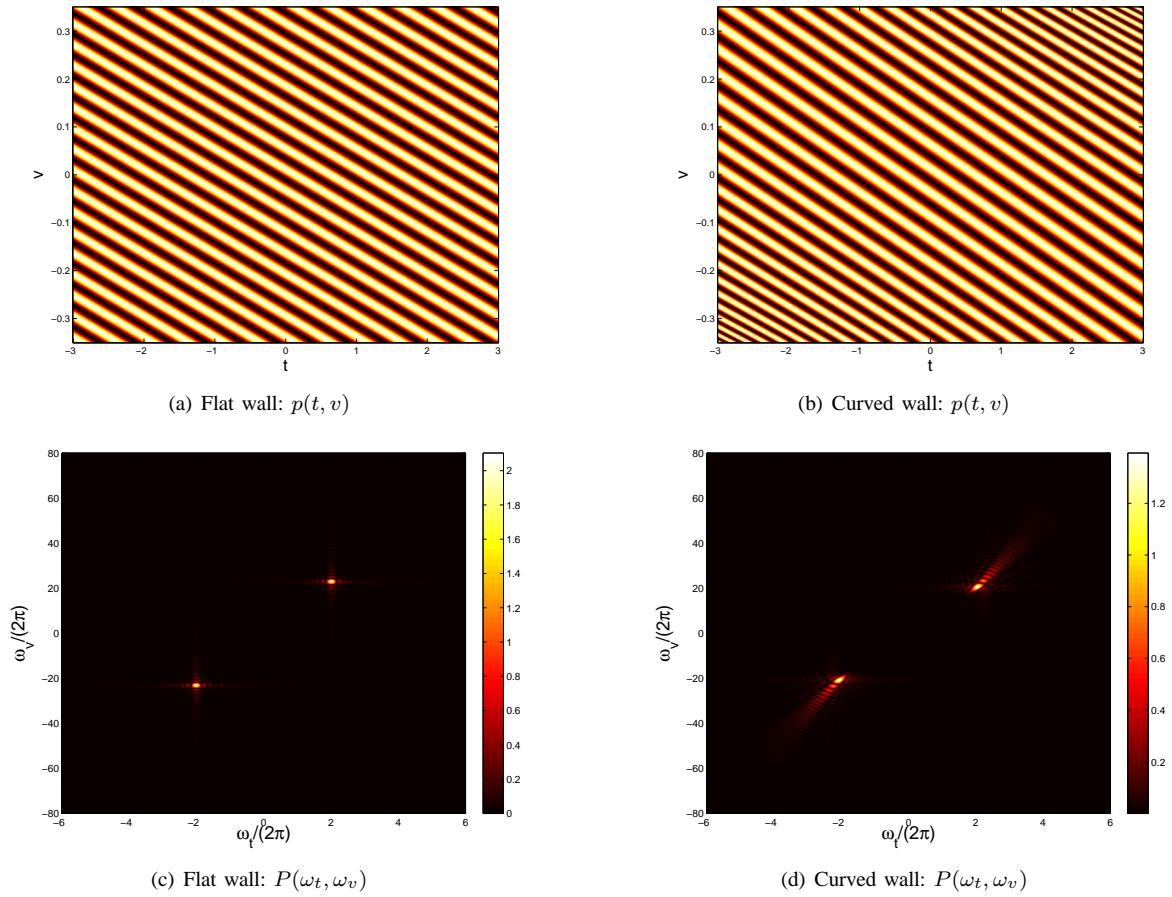


Fig. 6. Examples of the plenoptic function  $p(t, v)$  and its Fourier transform  $P(\omega_t, \omega_v)$  for flat and curved walls.

The corresponding change of variable in the space domain is

$$\begin{cases} t' = t, \\ v' = v + t/z_0. \end{cases}$$

Geometrically, this shearing operator maps, in the frequency domain, the line  $\omega_v = z_0\omega_t$  into the  $\omega_{v'}$  axis [i.e. from Figure 7(c) to Figure 7(d)]; or equivalently, in the space domain, it maps the  $t$  axis into the line  $v' = t'/z_0$  [i.e. from Figure 7(a) to Figure 7(b)]. Therefore, with a suitable choice of  $z_0$  such that  $z_{\min} \leq z_0 \leq z_{\max}$ , the spectrum of sheared POF is more compact along the  $\omega_{t'}$  axis. The optimal depth  $z_0$  suggested in [6] satisfies

$$\frac{1}{z_0} = \frac{1}{2} \left( \frac{1}{z_{\min}} + \frac{1}{z_{\max}} \right),$$

which can be obtained through Figure 3.

With the compact spectrum along the  $w_{t'}$  axis we can achieve high quality reconstruction (i.e. less aliasing) for the sheared POF by simply reconstructing along  $t'$  axis for each fixed  $v'$ . In other words, we interpolate the sheared POF along lines  $v' = v'_0$ . It is easy to see that corresponding to the line  $v' = v'_0$  in the sheared domain is the following line in the original domain [see Figure 7(a-b)]

$$v + t/z_0 = v_0 + t_0/z_0. \quad (31)$$

Therefore, equivalently, we can obtain high quality reconstruction of the original plenoptic function  $p(t, v)$  at a location

$(t_0, v_0)$  by interpolating along the line (31). From (1), we see that all corresponding light rays  $(t, v)$  that satisfy the line equation (31) intersect with the light ray  $(t_0, v_0)$  at a same point of depth  $z_0$ .

The Lumigraph [13] system employs the same reconstruction strategy which they call *depth correction* interpolation. The authors of [13] refer to the line (31) as an *optical flow* line (where the object surface “seen” by the light ray  $(t_0, v_0)$  is assumed to be at depth  $z_0$ ), and they expect the plenoptic function to be smooth along the optical flow lines. Their experiments show that reconstruction by depth-corrected interpolation along the optical flow lines has significantly higher quality compared to uncorrected interpolation (i.e. interpolate along same pixel lines  $v = v_0$ ).

We can characterize the smoothness of the plenoptic function along the optical flow line (31) by estimating the bandwidth of the 1D slice function of the POF along this line (which is also the 1D function along the line  $v' = v'_0$  of the sheared POF). The corresponding derivative for the bandwidth expanding factor in (22) is the *directional derivative* of  $s$  along the line (31) with the unit vector  $\mathbf{u} = (1, -1/z_0)$ . Using (12)-(13), we obtain the derivative of  $s$  in this direction as

$$\begin{aligned} D_{\mathbf{u}}s(t, v) &= \mathbf{u}_t \frac{\partial s(t, v)}{\partial t} + \mathbf{u}_v \frac{\partial s(t, v)}{\partial v} \\ &= \frac{(1 - z(x)/z_0) \sqrt{1 + (z'(x))^2}}{1 - v z'(x)}. \end{aligned} \quad (32)$$

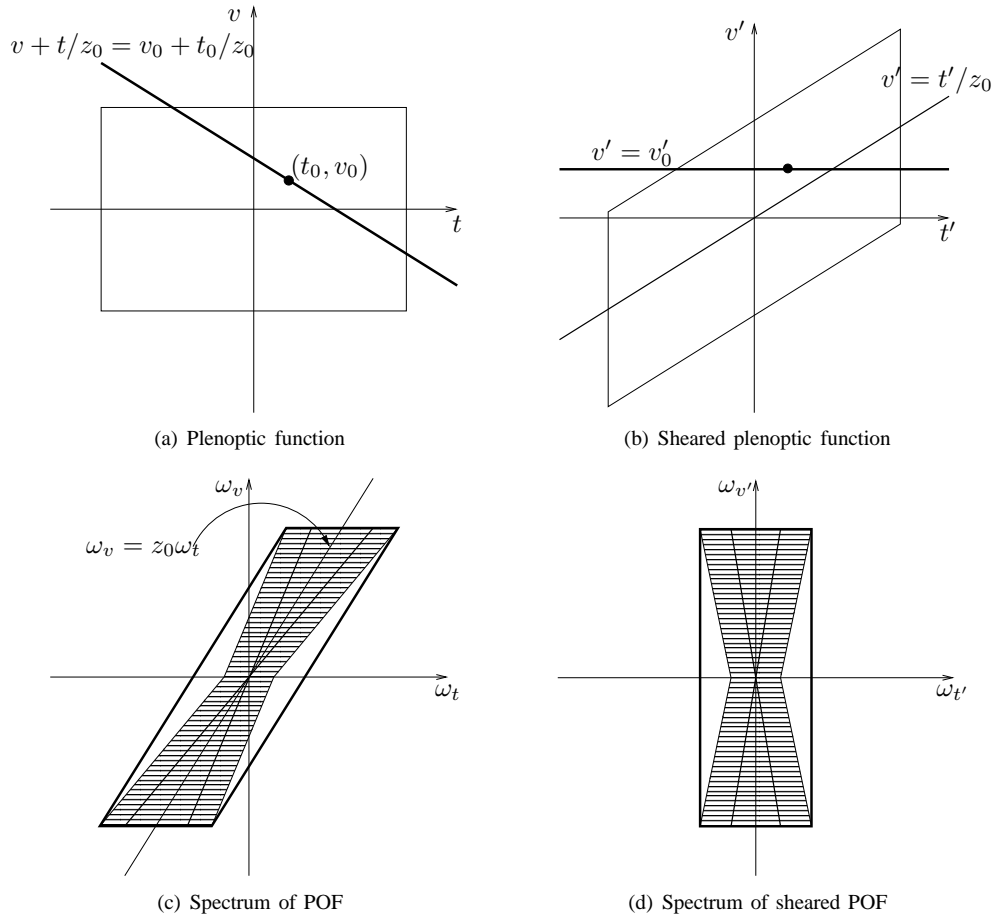


Fig. 7. Sheared spectrum of the plenoptic function by a change of variable:  $\omega_{t'} = \omega_t - (1/z_0)\omega_v$ ,  $\omega_{v'} = \omega_v$ . With appropriate choice of  $z_0$ , the sheared spectrum is most compacted near the  $\omega_{v'}$  axis.

Comparing  $D_{\mathbf{u}}s$  in (32) to  $\partial s/\partial t$  in (12), we see that, with a suitable choice of  $z_0$  such as  $z_0 = (z_{\min} + z_{\max})/2$ , the absolute value of the derivative of  $s$  in the direction  $\mathbf{u} = (1, -1/z_0)$  is smaller than the one in the direction  $(1, 0)$ . Hence, according to (22), the bandwidth of the POF along the optical flow line (31) is smaller than the bandwidth along the same pixel line  $v = v_0$ .

Figure 8 shows example slices of the POF for the *curved wall* scene described in Section VI along the same pixel line  $v = v_0$  and optical flow line (31) with  $t_0 = v_0 = 0$  and  $z_0 = 11.5$ . We see that the maximum frequency of the POF slice along the optical flow is much smaller compared to the one along the same pixel line, which confirms the advantage of depth-corrected interpolation in IBR. Using (12) and (32), and the surface depth and slope ranges for curved wall scene found in Section VI, we obtain estimates for the maximum frequency for these two slices of the POF as 3.2 Hz and 0.6 Hz, respectively. These estimates closely characterize the function plots in Figure 8.

### VIII. CONCLUSION

In this paper we studied the bandwidth of the plenoptic function of a simple scene model where a bandlimited signal is painted on a smooth surface. We show that in general the plenoptic function for this model is *not* bandlimited unless the

surface is flat. We then derive a simple rule to estimate the essential bandwidth, defined as the bandwidth where most of the signal energy resides, of the plenoptic function for this model. This essential bandwidth is estimated as the product of the bandwidth of the painted signal times the maximum absolute derivative of the surface curvilinear coordinate along a certain direction. Our analysis reveals that, in addition to the maximum and minimum surface depths, the bandwidths of the plenoptic function also depend on the maximum surface slope and maximum frequency of the painted signal. By treating the POF with a unifying formalism based on multidimensional signal processing, we can verify several important results, including induced filtering along the camera dimensions, depth correction interpolation in Lumigraph, and quantifying the necessary sampling rates. Numerical results show that the resulting estimated bandwidths of plenoptic functions are accurate and effectively characterize the performance of image based rendering algorithms.

**Acknowledgments.** The late David Slepian (1923 - 2007) and his seminal paper [25] have been inspirations for us in completing this paper. We also thank Nitin Aggarwal (UIUC) for the helpful discussions on the bandwidth of time-warped functions.

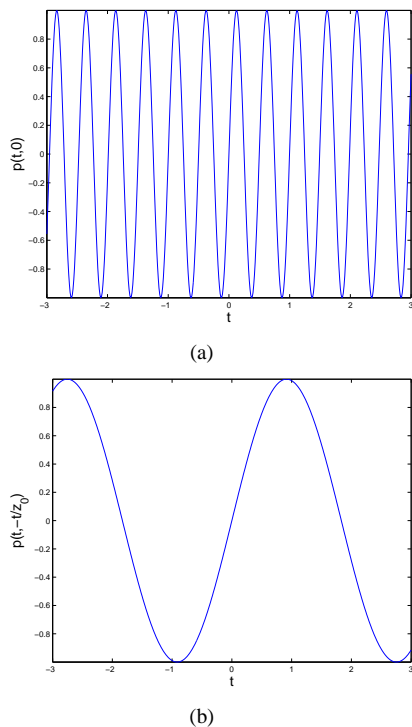


Fig. 8. Slices of the plenoptic function of the curved wall scene along: (a) same pixel line. (b) optical flow line with  $z_0 = 11.5$ .

## REFERENCES

- [1] L. McMillan and G. Bishop, "Plenoptic modeling: an image-based rendering system," in *Proc. SIGGRAPH*, 1995, pp. 39–46.
- [2] H.-Y. Shum, S. Kang, and S.-C. Chan, "Survey of image-based representations and compression techniques," *IEEE Trans. Circ. and Syst. for Video Tech.*, vol. 13, pp. 1020–1037, Nov. 2003.
- [3] C. Zhang and T. Chen, "A survey on image-based rendering – representation, sampling and compression," *EURASIP Signal Proc.: Image Commun.*, vol. 19, pp. 1–28, Jan. 2004.
- [4] H.-Y. Shum, S.-C. Chan, and S. B. Kang, *Image-Based Rendering*. Springer, 2007.
- [5] E. H. Adelson and J. R. Bergen, "The plenoptic function and the elements of early vision," in *Computational Models of Visual Processing*, M. Landy and J. A. Movshon, Eds. MIT Press, 1991, pp. 3–20.
- [6] J.-X. Chai, X. Tong, S.-C. Chan, and H.-Y. Shum, "Plenoptic sampling," in *Proc. SIGGRAPH*, 2000, pp. 307–318.
- [7] C. Zhang and T. Chen, "Spectral analysis for sampling image-based rendering data," *IEEE Trans. Circ. and Syst. for Video Tech.*, vol. 13, pp. 1038–1050, Nov. 2003.
- [8] F. Durand, N. Holzschuch, C. Soler, E. Chan, and F. X. Sillion, "A frequency analysis of light transport," in *Proc. SIGGRAPH*, 2005, pp. 1115–1126.
- [9] R. Ng, "Fourier slice photography," in *Proc. SIGGRAPH*, 2005, pp. 735–744.
- [10] A. Veeraraghavan, R. Raskar, A. Agrawal, A. Mohan, and J. Tumblin, "Dappled photography: Mask enhanced cameras for heterodyned light fields and coded aperture refocusing," in *Proc. SIGGRAPH*, 2007.
- [11] M. N. Do, D. Marchand-Maillet, and M. Vetterli, "On the bandlimit-ness of the plenoptic function," in *Proc. IEEE Int. Conf. on Image Proc.*, Genova, Italy, Sep. 2005.
- [12] M. Levoy and P. Hanrahan, "Light field rendering," in *Proc. SIGGRAPH*, 1996, pp. 31–40.
- [13] S. Gortler, R. Grzeszczuk, R. Szeliski, and M. Cohen, "The lumigraph," in *Proc. SIGGRAPH*, 1996, pp. 43–54.
- [14] O. D. Faugeras, *Three-Dimensional Computer Vision: A Geometric Viewpoint*. MIT Press, 1993.
- [15] R. C. Bolles, H. H. Baker, and D. H. Marimont, "Epipolar-plane image analysis: an approach to determining structure from motion," *International Journal of Computer Vision*, vol. 1, no. 7, pp. 7–55, 1987.
- [16] D. A. Forsyth and J. Ponce, *Computer Vision: A Modern Approach*. Prentice-Hall, 2002.
- [17] G. Miller, S. Rubin, and D. Ponceleon, "Lazy decompression of surface light fields for precomputed global illumination," in *Eurographics Rendering Workshop*, Vienna, Austria, 1998, pp. 281–292.
- [18] T. Ajdler, L. Sbaiz, and M. Vetterli, "The plenacoustic function and its sampling," *IEEE Trans. Signal Proc.*, vol. 54, no. 10, pp. 3790–3804, 2006.
- [19] D. Cochran and J. J. Clark, "On the sampling and reconstruction of time warped band-limited signals," in *Proc. IEEE Int. Conf. Acoust., Speech, and Signal Proc.*, Apr. 1990.
- [20] X.-G. Xia and Z. Zhang, "On a conjecture on time-warped band-limited signals," *IEEE Trans. Signal Proc.*, vol. 40, pp. 252–254, Jan. 1992.
- [21] S. Azizi, D. Cochran, and J. N. McDonald, "On the preservation of bandlimitedness under non-affine time warping," in *Proc. Int. Workshop on Sampling Theory and Applications*, Aug. 1999.
- [22] D. Marchand-Maillet, "Sampling theory for image-based rendering," Master's thesis, Swiss Federal Institute of Technology Lausanne, 2001.
- [23] B. P. Lathi, *Modern Digital and Analog Communication Systems*, 3rd ed. Oxford University Press, 1998.
- [24] G. Wolberg, *Digital Image Warping*. IEEE Computer Society Press, 1994.
- [25] D. Slepian, "On bandwidth," *Proc. IEEE*, vol. 64, no. 3, pp. 292–300, Mar. 1976.